Coupling acid neutralization and resource recovery to scale ocean alkalinity enhancement

Rocco D'Ascanio[1,2]*, Mojtaba Fakhraee[1,3], Nicolas Theunissen[1], Joachim A. R. Katchinoff[1,2], Matthew D. Eisaman[1,4], Noah J. Planavsky[1,4]

[1]Department of Earth and Planetary Sciences, Yale University, New Haven, CT, 06511
[2]CREW Carbon Inc., Brooklyn, NY, 11205
[3]Department of Earth Sciences, University of Connecticut, Storrs, CT, 06269
[4]Yale Center for Natural Carbon Capture, New Haven, CT, 06511

***Corresponding Author:** rocco.dascanio@yale.edu

Abstract

Ocean Alkalinity Enhancement (OAE) is a promising carbon dioxide removal (CDR) strategy with the theoretical potential to sequester gigatons of atmospheric CO_2 each year. Electrochemical OAE—where seawater alkalinity is increased by removing hydrochloric acid (HCl)—has attracted particular interest, but the viability of this approach at climate-relevant scales hinges on the development of low-cost, carbon-neutral strategies for HCl disposal. Here, we demonstrate a two-step bench-scale process that addresses this challenge by first neutralizing HCl using common mafic and ultramafic rocks, and then recovering valuable products from the resulting solutions. This process can yield co-products such as amorphous silica and nickel/cobalt hydroxides, while converting HCl into a saline solution that can be discharged to the ocean without reversing alkalinity gains. A technoeconomic case study in Washington State, USA, estimates the cost of acid neutralization at < $25 per tonne of CO_2 removed via OAE, with the potential for future net profitability as co-product purities improve.

Keywords

carbon dioxide removal, critical minerals, nickel, cobalt, precipitated silica

Synopsis

Ocean alkalinity enhancement is an emerging approach for removing carbon dioxide from the atmosphere, which could result in the production of significant amounts of acidic byproduct. Here, we propose a process which could treat this byproduct, while also recovering valuable materials such as nickel and cobalt.

Introduction

Anthropogenic greenhouse gas emissions, now exceeding 40 gigatonnes of CO_2 equivalents annually, have far-reaching consequences for ecosystems and human societies[1]. While decarbonizing the global economy is essential to curbing this trajectory, certain sectors will remain difficult to fully decarbonize. As a result, atmospheric carbon dioxide removal (CDR) is increasingly recognized as a necessary component of achieving global net-zero emissions[2]. When deployed at scale alongside rapid emissions reductions, CDR could help limit warming to below 2 °C by 2100, thereby reducing the most severe impacts of climate change[3].

Ocean alkalinity enhancement (OAE) is an emergent CDR technology which could supply a significant portion of the CDR required to limit global warming to 2 ºC [4,5]. In OAE, the total alkalinity of oceanic surface water is increased either via the addition of conservative base cations (i.e. Na^+, Mg^{2+}, Ca^{2+}) or via the removal of conservative anions (i.e. Cl^-, SO_4^{2-}). This alkalinity increase causes an instantaneous P_{CO2} deficit in the surface water, which drives mass transfer of CO_2 from the atmosphere into the surface ocean.

One commonly discussed pathway for ocean alkalinity enhancement is to use bipolar membrane electrodialysis to split seawater into a hydrochloric acid (HCl) stream and a sodium hydroxide (NaOH) stream—returning the NaOH to the ocean to enhance alkalinity[6,7]. A key advantage of this method is that it circumvents the need for external alkaline materials such as NaOH, $Ca(OH)_2$, or $Mg(OH)_2$, which are either geologically limited or produced through carbon-intensive processes[8,9]. In contrast to approaches that rely on mining or synthesizing these feedstocks, electrochemical OAE offers a more scalable pathway in terms of material inputs. However, this method faces some drawbacks, including the significant energy demands of electrodialysis and the need to manage the HCl byproduct[10].

The management of the HCl byproduct is a central challenge of electrochemical OAE. This issue is particularly critical given the massive quantities of HCl that could be produced at scale. For example, assuming complete air–sea CO_2 equilibration, the removal of one gigatonne (Gt) of atmospheric CO_2 would generate more than one Gt of distilled HCl—exceeding the current global HCl market by a factor of 50[11]. Improper disposal of this acid, especially if it is returned to the ocean, risks reversing the intended carbon removal by reducing seawater alkalinity. Thus, identifying carbon-neutral pathways for HCl disposal or neutralization is essential for the large-scale viability of electrochemical OAE[5].

Several methods have been proposed for the disposal or valorization of HCl produced via electrochemical OAE. Acid pretreatment of basaltic rocks has been shown to enhance CO_2 mineralization in silicate rocks by promoting the preferential release of cations such as Al, Fe, Ca, and Mg, which neutralize acidity and form silica-rich leached layers. The resulting cation-rich solutions may suppress secondary clay formation and increase the efficiency of CO_2 sequestration in basalt formations[12]. In another approach, low concentrations of HCl have been used to stimulate the growth of the microalgae *Picochlorum celeri* by converting bicarbonate in algal growth medium to dissolved CO_2, which is more readily transported across the cell membrane for utilization in photosynthesis. This effectively transforms acidity into algal biomass, with potential for carbon storage and further valorization, depending on the biomass end use[13]. Dissolution of olivine in hydrochloric acid has been used to produce high-purity $Mg(OH)_2$ for CO_2 sequestration, while also recovering silica and iron co-products, thereby unlocking added value from silicate minerals beyond

their carbon removal potential[14]. Other potential uses of carbon neutral acid include leaching of mine tailings for enhanced mineralization, and neutralization of toxic industrial byproducts[15,16].

Here, we expand upon pervious work and propose a method where neutralization of acidic OAE byproducts using silicate rocks is coupled to recovery of valuable co-products (Fig. 1). In the proposed process, ocean alkalinity enhancement is carried out by performing bipolar membrane electrodialysis on ocean water, resulting in a base stream which is returned to the ocean, and an acid stream which is neutralized using fine-ground silicate rocks:

$$4HCl_{(aq)} + M_{(2-X)}T_{(X)}SiO_{4(s)} \rightarrow (2\text{-}X)\ M^{2+}{}_{(aq)} + (X)\ T^{2+}{}_{(aq)} + 4Cl^{-}{}_{(aq)} + H_4SiO_{4(aq)} \quad (1)$$

Some of the cations released into solution during the silicate dissolution process are either valuable or unsuitable for discharge to the ocean (here, designated by T^{2+}, although in practice the oxidation state may vary). Following this step, valuable co-products and harmful contaminants can be precipitated from the neutralized acid solution via the addition of a small portion of the strong base generated for OAE:

$$(X)\ T^{2+}{}_{(aq)} + (2X)\ NaOH_{(aq)} + H_4SiO_{4(aq)} \rightarrow (2X)\ Na^{+}{}_{(aq)} + (X)\ T(OH)_{2(s)} + SiO_{2(s)} + 2\ H_2O_{(l)} \quad (2)$$

Performing reactions 1 and 2 in sequence converts HCl into a brine stream which can be returned to the ocean without counteracting the OAE process. Simultaneously, this process results in the generation of valuable precipitates, mainly SiO_2, iron oxides, and mixed hydroxide precipitates rich in critical elements. Coupled neutralization and resource recovery address the key externality of electrochemical OAE processes while harnessing a new revenue stream that can help drive adoption of this technology.

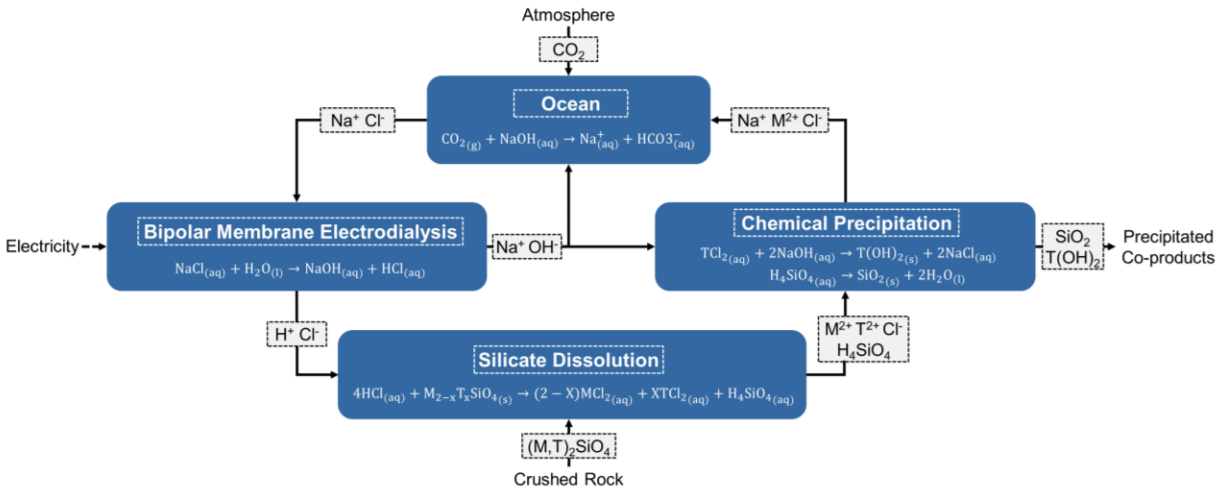

Figure 1. Flow diagram for the proposed process. NaCl derived from ocean water is split into NaOH and HCl streams by bipolar membrane electrodialysis. Then, HCl is neutralized using crushed silicate rocks, generating a neutralized acid solution rich in valuable metals. Co-products are precipitated from the neutralized acid stream using a small portion of the NaOH generated by electrodialysis, and the neutralized acid stream is returned to the ocean along with the remaining majority of the NaOH stream. M^{2+} denotes cations sourced from rock generally safe for discharge to the ocean (i.e. Mg^{2+}, Ca^{2+}) while T^{2+} denotes cations of interest for recovery for environmental or economic reasons (i.e. Fe^{2+}, Ni^{2+}, Co^{2+}).

Materials and Methods

Rock Samples

To explore the effect of mineral dissolution on modifying the pH of acidic water, three rock samples were explored in this study. Commercial fine ground olivine was sourced from Sibelco and mined at their site in Aheim, Norway. Another olivine sample was sourced from the Twin Sisters mine in Whatcom County, WA, USA. Fine ground basalt was also sourced from the Snider Rock Quarry in Port Angeles, WA, USA. Rock samples will be referred to as SB-OLV, TS-OLV and SR-BST for the Sibelco, Twin Sisters, and Snider Rock samples, respectively. The neutralized acids produced by reacting each feedstock with HCl will be referred to with the same names, followed by -NA.

Acid Neutralization Experiments

Batch acid neutralization experiments were performed in a 2 L Pyrex beaker. A JOANLAB OS-10L overhead mixer equipped with a PTFE-coated stirring rod was used to keep the beaker contents well-mixed, and the solution pH was monitored using an Orion™ Ross™ Sure-Flow™ glass bodied combination pH electrode connected to a Thermo Orion™ VSTAR12 Versa Star™ benchtop pH meter. The pH probe was calibrated daily using NIST-traceable pH 4.01, 7, and 10.01 Orion™ pH buffers from Thermo Scientific™. At the beginning of each experiment, 1 kg of fine-grained rock was added to the beaker, followed by 1 L of 0.9 N trace metal grade HCl. Reactor contents were mixed at approximately 240 RPM for the duration of the experiment. Fluid samples were collected through time for elemental analysis by filtering fluid through 0.22 micron polyethersulfone (PES) luer-lock syringe filters. After 4.5 hours, the mixer was turned off, and the beaker contents were allowed to settle for 15 minutes, after which the supernatant was decanted into a vacuum filtration system and filtered through a 0.22 micron PES filter.

Precipitation Experiments

Precipitation experiments were performed in the same benchtop apparatus as dissolution experiments, but equipped with a Thermo Scientific™ RT magnetic stirrer and a 3 in PTFE magnetic stir rod instead of the overhead mixer to better accommodate the range of fluid volume present in the beaker over the course of the experiment. A dropper funnel filled with NaOH (0.01 N for olivine samples, 0.1 N for basalt sample) was attached to a ring stand and situated directly above the beaker to allow for a slow addition of NaOH to the beaker contents. The dropper funnel and ring stand were placed on a scale to monitor the mass of NaOH dispensed over time. At the beginning of each experiment, 100 mL of neutralized acid and 100 mL of MilliQ® water were added to the beaker, and the stirring rate was set to approximately 100 RPM. The valve on the dropper funnel was opened, allowing NaOH solution to drip into the beaker. Fluid samples were collected and pH was measured through time following the same methodology as used in the acid neutralization experiments.

An additional precipitation experiment was performed only for TS-OLV-NA. This experiment was performed similarly to those described above, but the precipitation was paused, and the reactor contents were passed through a 0.22 micron PES vacuum filtration system at pH 5.75, 6.75, and 10.

Fluid Sample Analysis

Fluid samples were diluted into a solution of 1% trace metal grade nitric acid. Samples were analyzed for elemental concentrations using a Perkin Elmer Nexion 5000 multi-quadrupole inductively coupled plasma mass spectrometer, and a Perkin Elmer Avio 550 Max inductively coupled plasma optical emission spectrometer. Both instruments were calibrated prior to sample measurement using Perkin Elemer TruQ-MS multi-elemental calibration standard. Acid digested USGS-BHVO2 geochemical reference material was analyzed alongside samples during analytical runs as a quality control measure, with all measured USGS-BHVO2 concentrations within 8% of reported values[17].

Solid Phase Characterization

Precipitates were imaged using a Hitachi SU7000 scanning electron microscope, with an accelerating potential of 15 kV. Precipitates were also analyzed for major oxide composition by energy-dispersive x-ray spectroscopy (EDS), using an Oxford Instruments Ultim® Max 100 detector.

Technoeconomic Analysis

A techno-economic analysis (TEA) was performed for a case study of deploying the acid neutralization and co-product recovery process as an addendum to an electrochemical OAE processes in Washington State, USA. The system boundary for the TEA includes all capital and operating costs required for implementing the acid neutralization and co-product recovery processes – and intentionally omits all costs associated with the OAE process, such as acid base production costs, and costs of monitoring, reporting, and verification of carbon removal. This framework allows us to evaluate the stand-alone net profitability of neutralizing the acid stream and recovering the co-products as a potential method of hydrochloric acid byproduct management. As a starting point for this analysis, we assumed a gross CDR rate via electrochemical OAE, and calculated the respective acid production rate. The assumed feedstock for neutralization was TS-OLV. The key outcome of this analysis was the net profitability of acid neutralization and co-product recovery, per unit of gross CDR performed via OAE:

$$LPON = \frac{-NPV_{opex} - TCR}{R_{CDR} - E_{acid}} \quad (3)$$

where:
$LPON$ = levelized profit of neutralization and co-product recovery (USD $tCDR^{-1}$)
NPV_{opex} = net present value of operating expenditures (USD)
TCR = total capital requirement for project (USD)
R_{CDR} = gross carbon dioxide removed by OAE over project lifetime (tCDR)
E_{acid} = gross emissions from acid neutralization over project lifetime (tCO_2)

$LPON$ is the projected profit of the acid neutralization and co-product recovery process, per unit of gross CO_2 removal performed by the OAE deployment. The TCR is the sum of all up-front costs required to implement the proposed process. The net present value of operating expenditure (NPV_{opex}) accounts for all operating expenses and revenues over the project lifetime. NPV_{opex} is calculated using a discounted cash

flow analysis, which incorporates the time value of money by discounting future cash flows to their current value based on a discount rate.

The economic analysis for determining TCR and NPV_{opex} was carried out following recommendations from "A framework for techno-economic and life-cycle assessment in ocean alkalinity enhancement, Version 1.0", Section 7[18]. TCR first considers the bare erected costs of all process equipment, which was calculated based on quotes for comparable equipment and installation factors provided by the Enhanced Detailed Factor method[19]. Equipment costs were adjusted from available quotes using scaling and materials factors when required. TCR further incorporates engineering costs, process and project contingencies, start-up and owner's costs, and project financing costs (capital requirement factor)[20]. Future cashflows included in NPV_{opex} include the annual costs of crushed rock, labor, electricity, and waste disposal, and the annual revenue from sale of precipitates. By convention, when evaluating future cashflows, revenues were given a negative sign. Costs of crushed rock and labor were based on prior work in the enhanced weathering field, with rock costs inclusive of mining and production, grinding, and transport[21,22]. Cost of electricity and waste disposal was based on industrial rates for Washington state.

The results of the economic analysis were normalized to the gross – not net – CDR rate for the OAE process (R_{CDR}). The gross CDR rate was chosen as the functional unit because the lifecycle assessment of the OAE process was considered outside the scope of this work. However, we did account for additional emissions from acid neutralization by including $-E_{acid}$ in the denominator of equation 1. E_{acid} was calculated as the operating emissions of the acid neutralization process, and included emissions from producing and shipping crushed rock, disposing of waste, and electricity. This calculation omitted embodied emissions in process equipment, and emissions associated with offtake of products. By counting acid neutralization CO_2 emissions against OAE CO_2 removals, the acid neutralization process can be considered effectively CO_2 neutral.

Results and Discussion

Acid neutralization experiments

<u>pH increase during dissolution</u>

Our results show the selected feedstocks can play a major role in neutralizing strong acid from electrochemical OAE. For all rock samples, the pH of the acid solution was increased from a pH of approximately 0.2 to greater than 2 in 4.5 hours (Fig. 2a). This pH shift translates into >99% neutralization of the acidity that was present at the beginning of the experiment. For TS-OLV and SB-OLV, the pH increase is driven by the release of Mg^{2+} and Fe^{2+} into solution, while for SR-BST, the pH increase is predominantly attributed to Ca^{2+} and Al^{3+}, as well as Mg^{2+} and Fe^{2+}/Fe^{3+} to a lesser extent (Fig. 2b-d). Dissolution was non-stoichiometric for both olivine samples, with preferential release of Mg and Fe compared to Si. This is consistent with findings from others, who have observed that a divalent cation depleted surface layer can form during olivine dissolution, especially in acidic conditions where H^+ effectively swaps for divalent cations within the in the octahedral sites[23–25]. While not directly observed in our analyses, other studies have shown that cation depleted surface layers can polymerize into amorphous silica in excess of 10 nm thick[26]. Formation of a dissolution quenching surface layer could potentially be

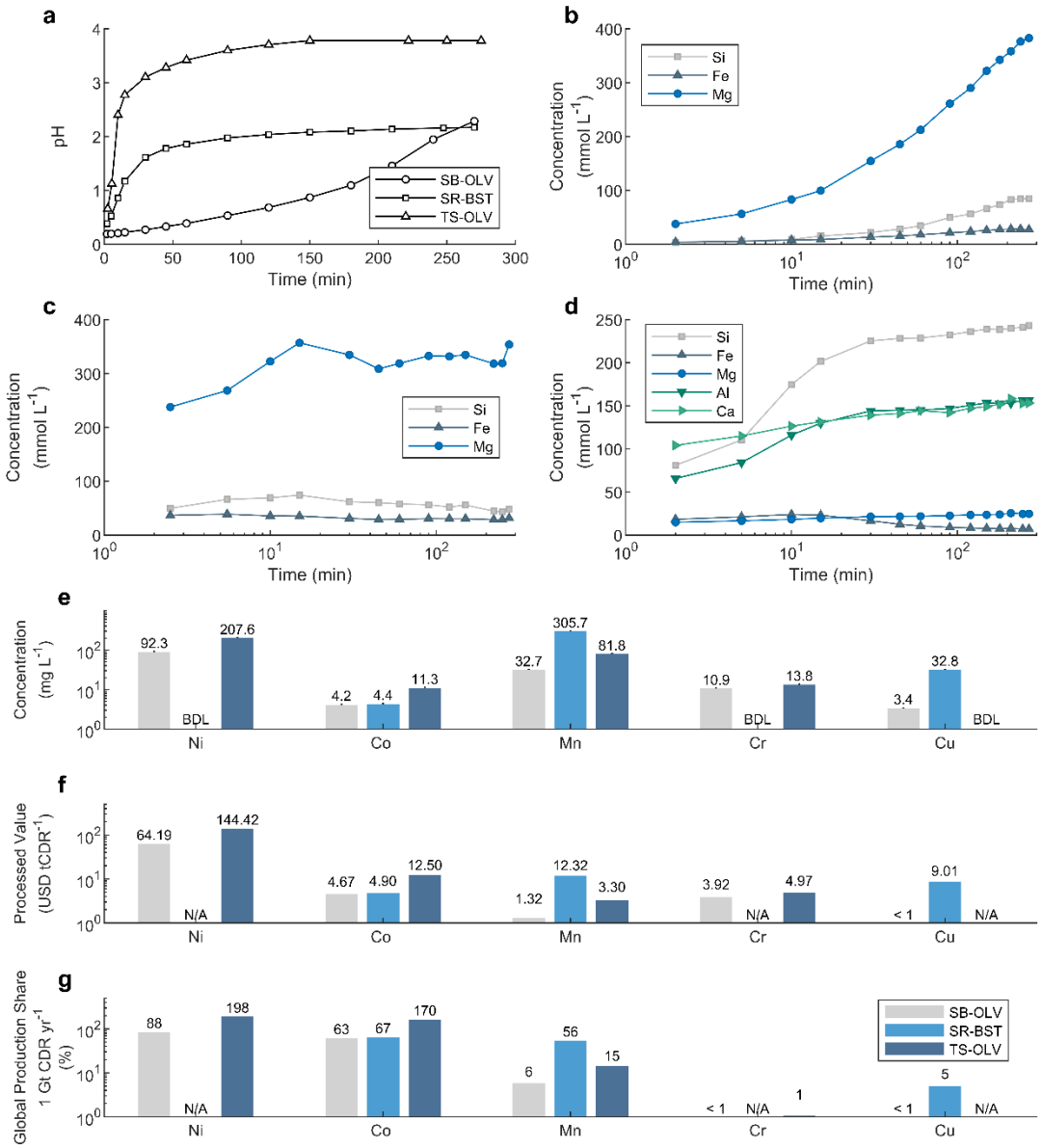

Figure 2. Results of acid neutralization experiments. **a:** pH through time during the acid neutralization reaction. **b, c, d:** concentrations of major cations and Si through time during acid neutralization reaction for SB-OLV, TS-OLV, and SR-BST, respectively. **e:** concentrations of valuable metals in neutralized acid solutions. **f:** economic value of metals if fully processed from neutralized acid solution into commodity metals. **g:** quantity of each metal released into neutralized acid if feedstocks were used to neutralize the acid produced by 1 Gt CDR, as a percentage of the 2023 global mine production for each metal.

further enhanced in batch reaction systems, where particle surfaces are in prolonged contact with solution which is oversaturated with respect to amorphous silica, which could drive precipitation onto polymerized SiO_2 surfaces (neutralized acids ranged from 20 to nearly 200 times supersaturated with respect to

amorphous silica)[27]. This warrants further work exploring passivation during prolonged silicate dissolution reactions in HCl, especially considering that passivation of olivine surfaces during mineral carbonation process is well established, often leading to significant declines in reaction kinetics and sometimes functionally incomplete reactions[28,29]. Nonetheless, these findings highlight the efficiency of freshly crushed silicate rocks for neutralizing strong acids, despite additional research needed into methods of minimizing surface passivation of the feedstock during dissolution.

Fluxes and value of critical elements released into neutralized acid solution

All three feedstocks released significant quantities of valuable metals into neutralized acid solutions. Most notably, olivine samples released Ni in concentrations ranging from 90 to >200 mg L^{-1}, Co ranging from 4 to 11 mg L^{-1}, and Cr ranging from 11 to 14 mg L^{-1} (Fig. 2e). Ni and Cr concentrations for the basalt sample were below the detection limit for the method, but basalt did release significant Co, and greatly elevated Mn and Cu compared to olivine samples.

Ni, Co, Cr, Mn, and Cu are key elements relevant to battery technology and the renewable energy transition[30]. Besides Cu, all these elements were included in the 2022 U.S. Critical Minerals List published by the U.S. Geological Survey[31]. The US Department of Energy (DOE) has also emphasized the importance of Ni and Co to the US energy infrastructure, with Ni and Co both rated as critical over the decade 2025 to 2035[32]. Ni is widely used in stainless steel, specialty alloys, and cathode materials for lithium-ion batteries, the latter of which are facing rapid growth in demand due to growth in the electric vehicle and grid level energy storage industries. Similarly, Co criticality is tied to its use in superalloys and a variety of battery technologies[33].

Among the critical elements released into neutralized acid, Ni recovery presents the largest opportunity for value addition. Considering the acid production rate per unit CDR for an electrochemical OAE deployment, and the concentrations of Ni in TS-OLV-NA and SB-OLV-NA, the quantity of nickel released during acid neutralization is valued at $144 and $64 USD per tonne CDR ($tCDR^{-1}$), assuming full processing into metallic Ni (Fig. 2f). Furthermore, TS-OLV could serve as an enormous domestic source of Ni and Co for the U.S. We estimate that if TS-OLV was used to neutralize acid produced by electrochemical OAE with a deployment rate of one Gt CDR per year, the total Ni and Co releases would be 198% and 170% of the current global production rates of these metals (Fig. 2g). Deploying electrochemical OAE and acid neutralization at this scale would likely not be rock limited, as this this would require 1.2 Gt of TS-OLV per year (assuming stoichiometric dissolution), but it is estimated that the Twin Sisters dunite body, which covers over 36 square miles, contains in excess of 200 Gt of dunite[34,35]. As additional context, the global consumption rate of crushed stone for concrete and road aggregates is 11.3 Gt of rock a year[36]. Building domestic production capacity for Ni and Co could have considerable geopolitical implications for nations that rely on global supply chains[37–40]. It is also important to note that besides the potential for value addition, recovery of these metals is crucial as many are aquatic contaminants that can be toxic to marine life[41–43].

Precipitation experiments

We evaluated chemical precipitation as a pathway to recovering valuable metals from neutralized acid solution. This recovery method was chosen because NaOH would theoretically be available as a

precipitating agent at electrochemical OAE sites, provided that the NaOH draw for precipitation is minimal. The ideal outcome during precipitation would be recovery of high purity metal oxide or hydroxide precipitates for most elements (Si, Al, Fe, Ni, Co, Cr, Mn, Cu), while leaving major base cations (Ca, Mg, Na) in solution to continue to charge balance Cl^-. Secondary goals of the precipitation process include adjusting the pH to an acceptable discharge level (5-9 for most nationally regulated permits) and removing as many toxic metals from the neutralized acid stream as possible. We monitored for precipitation of metals from neutralized acid by measuring the concentrations of dissolved metal cations in neutralized acid solution as the pH was steadily increased using a continuous feed of NaOH.

Co-product recovery via NaOH addition

In these experiments, Na^+ replaces metal cations in neutralized acid solution as metal oxides and hydroxides precipitate, as expected based on chemical precipitation theory[43]. In Figure 3a-c, decreases in concentration of dissolve species as pH increases are attributed to precipitation. For SB-OLV-NA, Si and Fe co-precipitated from solution between pHs 6 and 7, and Ni, Mn, and Co co-precipitated from solution between pHs 7 and 9 (Fig. 3a). TS-OLV-NA displayed a similar window for recovery of mixed Ni, Mn, and Co precipitates, but a greater potential for separation of Si and Fe, with Si precipitating almost entirely before pH 6 (Fig 3b). Both SB-OLV-NA and TS-OLV-NA displayed minimal Mg precipitation, which is a desirable outcome as Mg charge balances the majority of the Cl^- present in solution. SR-BST-NA displayed poor separation potential, with Si, Al, and Fe co-precipitating between pH's 3 and 5.5, and Mn, Mg, and Ca co-precipitating between pH's 6 and 10 (Fig 3c). However, SR-BST-NA did selectively precipitate Cu between pH's 4.5 and 6.5.

These results suggest that, from a metal recovery point of view, olivine feedstocks are superior to basalts for co-product recovery via chemical precipitation with NaOH. The precipitates generated from the olivine neutralized acid samples between pH 7 and 9 should be rich in Ni, with lesser amounts of Mn and Co co-precipitated. Conversely, the more complex matrix of the basalt neutralized acid and the lack of Ni made recovery of critical elements a challenge with this feedstock. However, the extensive supply of Cu rich basaltic mine tailings—some of which are currently causing environmental damage—provides justification for further work on acid neutralization and metal recovery using basalts[44]. Beyond critical elements, TS-OLV is likely the superior feedstock for this process owing to the difference in pH between when Si and Fe precipitate from TS-OLV-NA, which should allow for independent recovery of SiO_2 and Fe_2O_3.

Inefficiencies attributed to NaOH use for precipitation

It is also crucial to consider the amount of NaOH consumed during precipitation, as this consumption would directly decrease the CDR rate for the associated electrochemical OAE deployment. For SB-OLV-NA and TS-OLV-NA, a large portion of the NaOH consumption occurs between pH 5.5 and 6.5 (Fig 3d,e), chiefly attributed to precipitation of Fe from solution. For SR-BST-NA, much more NaOH is consumed compared to the olivine samples, with most consumption occurring between pH 2 and 5 (Fig. 3f). This corresponds to the pH range where Al and Fe precipitate from SR-BST-NA. In practice, the exact inefficiency incurred by consumption of NaOH will depend on the chosen ending pH of the precipitation process. To estimate this inefficiency, we selected optimum endpoints of precipitation for each sample, demonstrated by the dotted grey lines in Fig. 3d-f. These endpoints were selected because they represent the pHs at which there

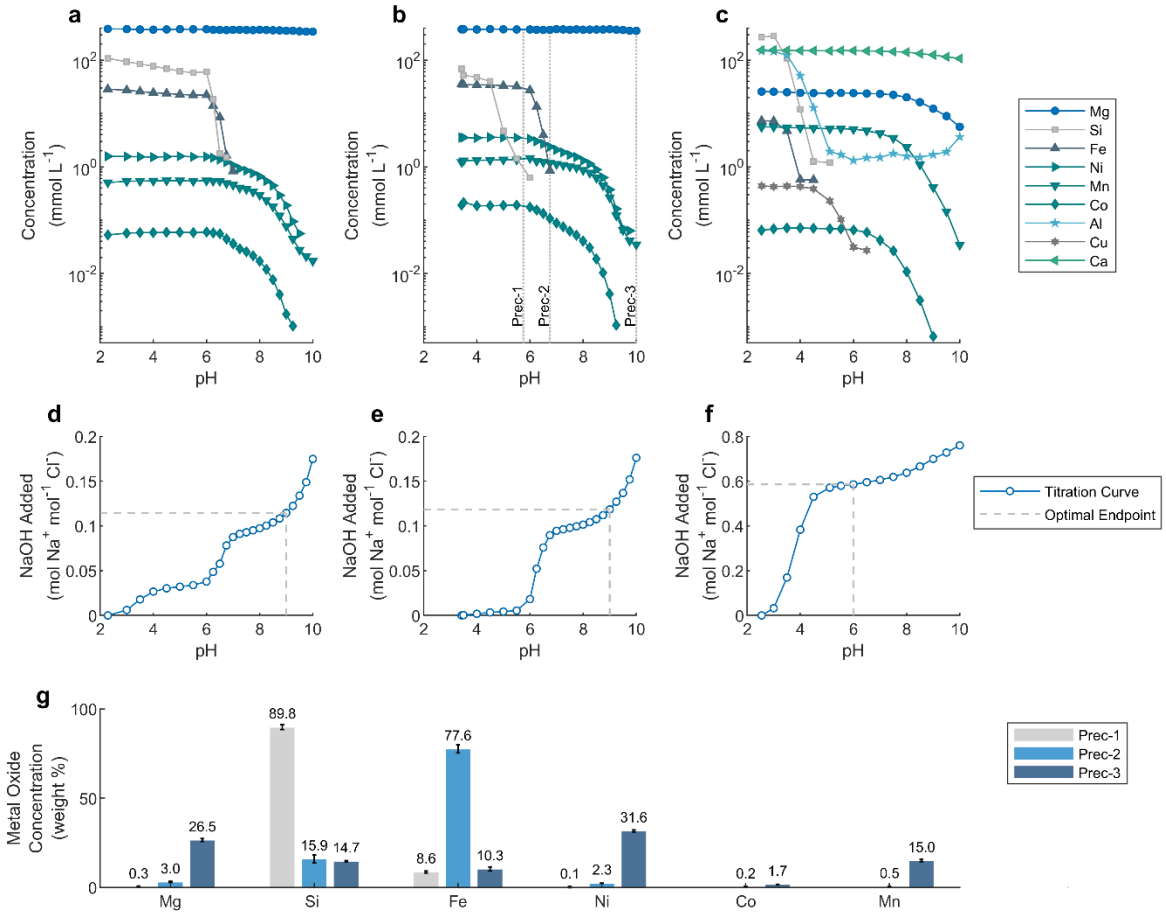

Figure 3. Results of precipitation experiments. **a, b, c**: concentrations of dissolved metals in neutralized acid throughout the NaOH addition experiments, for SB-OLV-NA, SR-BST-NA, and TS-OLV-NA, respectively. Decreases in concentration as pH increases are attributed to precipitation of each species. For TS-OLV-NA, a second experiment was performed where precipitates were recovered from solution via vacuum filtration at three different pHs, indicated by the dotted lines labeled Prec-1, Prec-2, and Prec-3. **d, e, f**: titration curves demonstrating the quantity of NaOH added per mole of Cl^- in solution during precipitation for SB-OLV-NA, SR-BST-NA, and TS-OLV-NA respectively. Grey dotted lines represent theoretical optimal endpoints for NaOH addition, optimizing across element recovery, major cation precipitation, and final pH. **g:** elemental composition for the three sequential precipitates generated from TS-OLV-NA, measured using EDS. Precipitates 1, 2, and 3 appeared rich in silica, iron oxide, and nickel oxides/hydroxides respectively.

is near-complete Ni recovery for SB-OLV-NA and TS-OLV-NA, and near-complete Cu recovery for SR-BST-NA. Additionally, SR-BST-NA begins to precipitate Mg and Ca at higher pHs, which is an undesirable outcome. The NaOH required to achieve these endpoints, as a percentage of the theoretical NaOH generated when producing the HCl, is 11.4%, 11.8% and 58.8%, for SB-OLV-NA, TS-OLV-NA, and SR-BST-NA, respectively.

The greatly elevated NaOH consumption by the basalt neutralized acid is a direct outcome of the composition of the crushed rock feedstock. Greater than 50% of the cation equivalents released by SR-BST

during neutralization are Al and Fe, whereas these elements account for less than 10% of the cation equivalents released by SB-OLV and TS-OLV. The presence of Al and Fe in neutralization feedstock can be a major drawback, as these cations will readily enter solution at low pH (<2), driving the pH increase and the quenching the dissolution reaction, but will then almost certainly be precipitated from solution when re-adjusting neutralized acid from pH ~2 to an acceptable discharge pH. Conversely, the presence of major cations (Mg, Ca, Na) in neutralization feedstock is advantageous, as these cations neutralize acid but only precipitate at much higher pHs, allowing them to continue to charge balance Cl^- in the final brine stream. The presence of Al and Fe could be advantageous if they are precipitated independently as valuable Al_2O_3 and Fe_2O_3 co-products, but in the case of SR-BST-NA, these elements are co-precipitated, and the value of the mixed precipitate is questionable. This result underscores the importance of rock composition for our process, and suggests that the complex elemental matrix of basalts may render them less effective for chemical precipitation using NaOH.

Precipitate analysis via EDS

Following the initial precipitation experiments, we performed an additional experiment where precipitates were recovered from TS-OLV-NA solution at various pHs via vacuum filtration. This approach provided a more detailed understanding of precipitate bulk elemental composition compared to the initial experiments, allowing for a more meaningful comparison of precipitates to commercial products, and a better parameterization of our techno-economic model. Only TS-OLV-NA was selected for this analysis, due to its superior apparent separation potential between Si, Fe, and Ni. By pausing the NaOH addition to TS-OLV-NA and filtering out the precipitated solids at pH's 5.75, 6.75, and 10, three precipitates were generated, referred to as Prec-1, Prec-2, and Prec-3, respectively (see Fig. 3b).

This analysis establishes that precipitates can be compositionally similar to commercial products. Bulk elemental concentration of the precipitates measured by EDS mirrors what is expected based on the initial precipitation experiments, with Prec-1 being Si rich, Prec-2 Fe rich, and Prec-3 Ni rich (Fig. 3g). Prec-1 is nearly 90% SiO_2 with the balance of the composition being nearly all Fe oxides, making Prec-1 similar to a low-grade precipitated amorphous silica. Prec-2 is similar in composition to iron ore, at 78% Fe oxides with the balance composed of SiO_2 and a small amount of Ni oxide. Prec-3 contains nearly all the Ni, Co, and Mn precipitated from solution, with a composition of 32% Ni oxide, 15 % Mn oxide, 1.7 % Co oxide, and the balance Si, Fe, and Mg oxides. Prec-3 is most similar to mixed hydroxide precipitate (MHP) – a Ni, Co, and Mn-rich intermediate commonly produced during high pressure acid leaching of nickel limonite and saprolite ores[45]. However, Prec-3 is slightly lower in Ni than commercial MHP, which is typically around 45-50% Ni oxide[46–48].

Techno-Economic Analysis

We conducted a techno-economic analysis (TEA) to evaluate the extent to which the recovered precipitates could offset the costs of the proposed acid neutralization and precipitation process at a site in Washington State, USA. In the baseline scenario, we assumed that crushed olivine would be transported by truck from the Twin Sisters Mine in Whatcom County, WA to a coastal facility in Anacortes, WA. At the facility, acid from electrochemical OAE is neutralized using crushed rock, and co-products are recovered by chemical precipitation using NaOH. Prec-1 and Prec-2 were assumed to be marketable as precipitated amorphous

silica and iron ore, respectively. Prec-3 was considered as MHP. To compensate for lower purity in our benchtop products compared to commercial standards, we applied discounted market values, pricing silica and MHP at approximately 20% and 60% of their typical market prices, respectively. Further details on the process model and TEA parameterization are provided in the supplement (Table S1 and Figure S1).

Process economics and sensitivity

Despite the value recovered from product streams, acid neutralization under baseline conditions will still impose a net cost to OAE project developers. With the assumed baseline prices for the co-products, which reflect the purity of the precipitates obtained in this work, the levelized profit of neutralization (LPON) is –23 USD $tCDR^{-1}$. The overall cost is largely driven by operating expenditures, which outweigh the total capital requirement when amortized over the project lifetime. Capital costs are relatively evenly distributed across the different stages of project development (Fig. 4a), while the dominant operating expenses arise from sourcing crushed rock and labor for process operation (Fig. 4b). Revenues from co-products, particularly mixed hydroxide precipitate (MHP), offset a significant portion of operating costs but are not sufficient to render the process profitable under current assumptions.

To explore the economic robustness of the process, we conducted a sensitivity analysis on key parameters affecting the LPON (Fig. 4c). Among all the factors, the dissolution efficiency—the fraction of olivine that dissolves before surface passivation—exerted the strongest leverage on the cost. At the lower bound dissolution efficiency of 50%, the LPON dropped substantially to -77 USD $tCDR^{-1}$, underscoring the sensitivity of many individual costs (e.g. mining and grinding rock, transporting rock and disposing of waste) to reaction completeness. Market prices for silica and MHP were also major cost drivers, highlighting that the process could become net profitable (positive LPON) if the precipitates can command prices comparable to higher-purity commercial products. Particularly, achieving a silica co-product analogous to commercial precipitated amorphous silica, for use in applications such as reinforcement of rubber and plastics, could be transformational for the process unit economics, resulting in an LPON of 23 USD $tCDR^{-1}$ [49]. This result accentuates the importance of refining precipitate purity as an avenue of future work. The cost of extracting rock was another important driver, in line with many geochemical carbon removal approaches[22].

The improvements in precipitate purity which are required to achieve a net-profitable process could potentially be realized by further lab scale experimentation and process modifications. One approach to increased purity could be narrowing the pH range over which each precipitate is recovered. Results displayed in Fig. 3b suggest that this approach could likely help minimize Fe content in Prec-1 and Mg content in Prec-3, potentially resulting in materials that are >95% SiO_2 and >40% NiO, respectively. Other process modifications, such as washing of Prec-1 with HCl to decrease Fe content, and use of selective or different precipitating agents for Ni and Co recovery, could also potentially result in substantially higher purities[50–52].

Carbon intensity of co-products

An important dimension of this process is that the co-products—nickel and cobalt hydroxides, iron ore, and amorphous silica—can be considered effectively carbon neutral, as the emissions associated with their

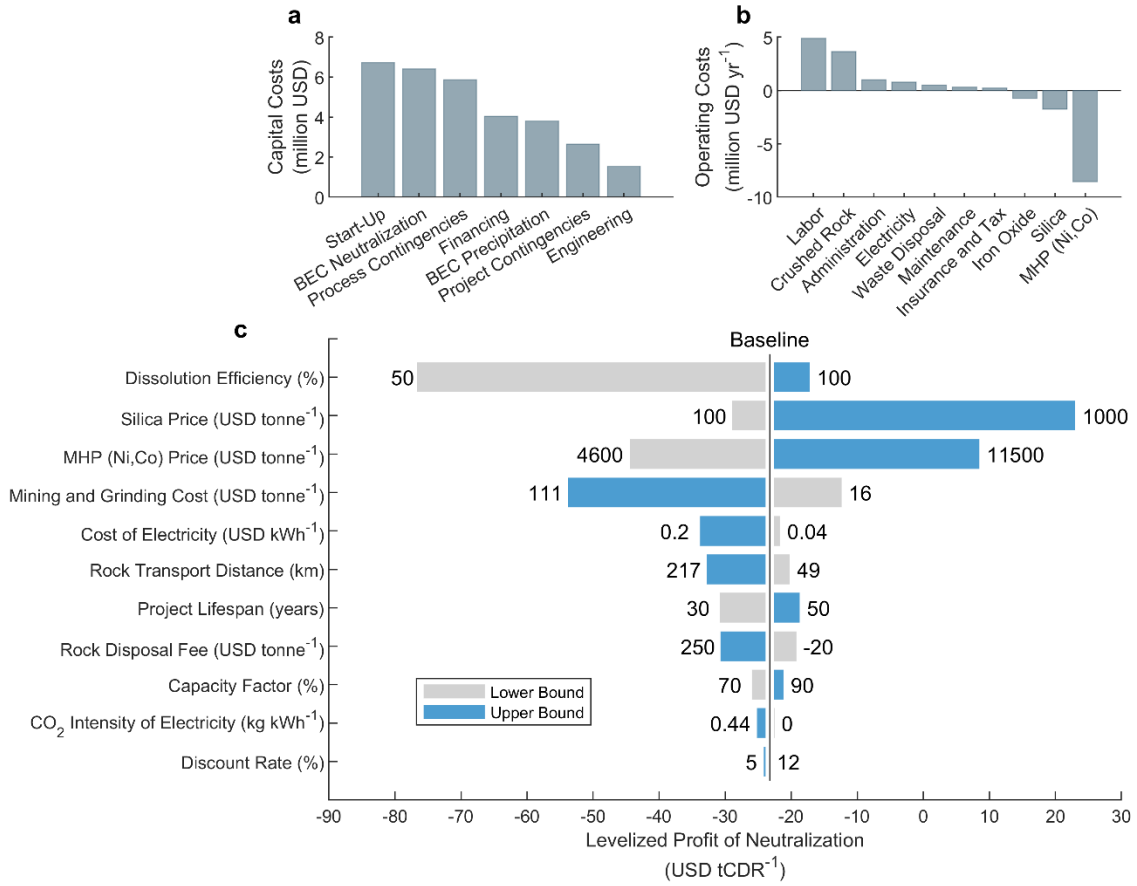

Figure 4. Results of technoeconomic analysis case study of acid neutralization and co-product recovery in Washington state, USA. **a:** Breakdown of total capital requirement for base case scenario. **b:** Breakdown of operating costs (cost and revenue streams) for base case scenario. Revenue streams are displayed as negative values. **c:** Results of sensitivity analysis, where parameters listed on the y-axis were varied from their base values to an upper and lower bound, resulting in changes in the levelized profit of neutralization. Numbers within plot area are the upper and lower bound values for each sensitivity parameter.

production are counted against the CDR performed by the OAE project. In our base case scenario, these emissions amounted to 11.1% of the gross CDR rate for the OAE deployment. It is likely that this accounting approach would be used in practice, as to qualify for carbon removal registries, projects must meet rigorous lifecycle assessment standards that comprehensively account for all emissions related to the carbon removal pathway (e.g., Ocean Alkalinity Enhancement from Coastal Outfalls v1.0 published by Isometric). In the case of electrochemical OAE with acid neutralization, emissions associated with the neutralization and co-product recovery process, including emissions from mining, rock processing, rock transport, and electricity, would be included within this scope. As a result, the emissions from these operations would be deducted from the total CO_2 removal credited to the OAE project, making the resulting co-products carbon neutral.

This stands in sharp contrast to conventional production methods for these materials, which are often highly carbon-intensive. For example, life cycle assessments have estimated the global warming potential of nickel

sulfate hexahydrate (NSH) produced via high pressure acid leaching processes at 36.8 kg CO_2 equivalents (CO_2eq) per kilogram of NSH[53]. 52% of these emissions are attributable to production of the unpurified MHP, amounting to 19.1 kg CO_2eq per kg NSH. Replacing high pressure acid leaching process with our approach for producing MHP could effectively eliminate these emissions. However, it is important to note that the high pressure acid leaching processes only accounts for a lesser fraction of global Ni production, and that other processes for producing NSH or metallic Ni can be more or less emissions intensive than this pathway[54].

Silica (e.g., precipitated silica, silica sand) and iron ore production also carry significant emissions footprints due to chemical processing and mining operations[55–58]. Therefore, if the carbon-neutral variants produced via this process were to enter commodity markets at scale, they could displace more carbon-intensive supply chains—resulting in avoided emissions that are additional to the credited carbon removal. Crucially, this outcome would require further work to develop co-products from this process that meet precise commercial specifications for elemental purity, particle size, specific surface area, and other chemical characteristics.

Conclusions

In this work, we propose a viable pathway for mitigating a major externality of electrochemical ocean alkalinity enhancement (OAE)—hydrochloric acid—while simultaneously recovering valuable resources from silicate rocks. Our results highlight the potential for this approach to generate carbon-neutral co-products such as amorphous silica, mixed hydroxide precipitate (MHP), and iron ore, with market applications that could offset process costs and offer additional climate benefits through the displacement of carbon-intensive conventional materials.

Techno-economic analysis (TEA) underscores several key hurdles to scaling this approach. Most notably, the extent of rock dissolution directly influences many of the operating expenditures, making reduced dissolution from feedstock passivation a critical bottleneck influencing the unit economics of the process. Future work should focus on investigating potential decay in reaction kinetics with feedstock re-use, and if necessary, strategies to enhance or prolong reaction kinetics including possible surface treatments or process modifications. Additionally, another key cost driver was the commercial value of the silica and MHP co-products, which is tightly linked to their purity. Advancing product refinement—particularly to meet specifications for high-grade silica and MHP—could transform the process from cost-negative to economically self-sustaining.

Beyond its relevance to electrochemical OAE, our proposed approach may have broader implications for other settings where acidic waste streams pose environmental and climate risks. For example, acid mine drainage and acidic industrial effluents could potentially drive release of biogenic CO_2 from natural ecosystems and are often treated with carbonate-based neutralizers, some of which can release CO_2 during the neutralization process[59]. Substituting silicate-based neutralization could avoid these emissions while enabling co-product recovery. Deploying this technology in such legacy or distributed systems may offer near-term opportunities for scale-up, providing an opportunity to transition to a more widespread deployment as the carbon removal and OAE industries grow.

Together, these findings suggest that mineral-based acid neutralization can not only serve as a critical step to be coupled to electrochemical OAE, but also as a potentially scalable, multifunctional climate solution with value across both emerging and established industrial sectors.

Supporting Information

Additional details on technoeconomic model parameterization, and process model mass and energy flows (DOCX).

Acknowledgments

The authors thank the Carbon to Sea initiative for support in funding this research. N.P.J. acknowledges support from the Yale Center for Nature Carbon Capture. This research made use of the Yale Analytical and Stable Isotope Center at Yale University, and R.D. acknowledges support from Jonas Karosas in operating the ICP-MS and ICP-OES. The authors are also deeply grateful for the contributions of late co-author Matthew Eisaman who passed away in early 2025, particularly for his vision in guiding this research and the broader field of ocean alkalinity enhancement.

Funding

All work carried out for this publication was funded by a technology development grant from the Carbon to Sea initiative, and by the Yale Center for Nature Carbon Capture.

References

(1) Calvin, K.; Dasgupta, D.; Krinner, G.; Mukherji, A.; Thorne, P. W.; Trisos, C.; Romero, J.; Aldunce, P.; Barrett, K.; Blanco, G.; Cheung, W. W. L.; Connors, S.; Denton, F.; Diongue-Niang, A.; Dodman, D.; Garschagen, M.; Geden, O.; Hayward, B.; Jones, C.; Jotzo, F.; Krug, T.; Lasco, R.; Lee, Y.-Y.; Masson-Delmotte, V.; Meinshausen, M.; Mintenbeck, K.; Mokssit, A.; Otto, F. E. L.; Pathak, M.; Pirani, A.; Poloczanska, E.; Pörtner, H.-O.; Revi, A.; Roberts, D. C.; Roy, J.; Ruane, A. C.; Skea, J.; Shukla, P. R.; Slade, R.; Slangen, A.; Sokona, Y.; Sörensson, A. A.; Tignor, M.; Van Vuuren, D.; Wei, Y.-M.; Winkler, H.; Zhai, P.; Zommers, Z.; Hourcade, J.-C.; Johnson, F. X.; Pachauri, S.; Simpson, N. P.; Singh, C.; Thomas, A.; Totin, E.; Arias, P.; Bustamante, M.; Elgizouli, I.; Flato, G.; Howden, M.; Méndez-Vallejo, C.; Pereira, J. J.; Pichs-Madruga, R.; Rose, S. K.; Saheb, Y.; Sánchez Rodríguez, R.; Ürge-Vorsatz, D.; Xiao, C.; Yassaa, N.; Alegría, A.; Armour, K.; Bednar-Friedl, B.; Blok, K.; Cissé, G.; Dentener, F.; Eriksen, S.; Fischer, E.; Garner, G.; Guivarch, C.; Haasnoot, M.; Hansen, G.; Hauser, M.; Hawkins, E.; Hermans, T.; Kopp, R.; Leprince-Ringuet, N.; Lewis, J.; Ley, D.; Ludden, C.; Niamir, L.; Nicholls, Z.; Some, S.; Szopa, S.; Trewin, B.; Van Der Wijst, K.-I.; Winter, G.; Witting, M.; Birt, A.; Ha, M.; Romero, J.; Kim, J.; Haites, E. F.; Jung, Y.; Stavins, R.; Birt, A.; Ha, M.; Orendain, D. J. A.; Ignon, L.; Park, S.; Park, Y.; Reisinger, A.; Cammaramo, D.; Fischlin, A.; Fuglestvedt, J. S.; Hansen, G.; Ludden, C.; Masson-Delmotte, V.; Matthews, J. B. R.; Mintenbeck, K.; Pirani, A.; Poloczanska, E.; Leprince-Ringuet, N.; Péan, C. *IPCC, 2023: Climate Change 2023: Synthesis Report. Contribution of Working Groups I, II and III to the Sixth Assessment Report of the Intergovernmental Panel on Climate Change [Core Writing Team, H. Lee and J. Romero (Eds.)]. IPCC, Geneva, Switzerland.*, First.; Intergovernmental Panel on Climate Change (IPCC), 2023. https://doi.org/10.59327/IPCC/AR6-9789291691647.

(2) *Climate Change 2022: Mitigation of Climate Change*; Shukla, P. R., Skea, J., Reisinger, A. R., IPCC, Eds.; IPCC: Geneva, 2022.

(3) Rogelj, J.; Popp, A.; Calvin, K. V.; Luderer, G.; Emmerling, J.; Gernaat, D.; Fujimori, S.; Strefler, J.; Hasegawa, T.; Marangoni, G.; Krey, V.; Kriegler, E.; Riahi, K.; van Vuuren, D. P.; Doelman, J.; Drouet, L.; Edmonds, J.; Fricko, O.; Harmsen, M.; Havlík, P.; Humpenöder, F.; Stehfest, E.; Tavoni, M. Scenarios towards Limiting Global Mean Temperature Increase below 1.5 °C. *Nature Clim Change* **2018**, *8* (4), 325–332. https://doi.org/10.1038/s41558-018-0091-3.

(4) Renforth, P.; Henderson, G. Assessing Ocean Alkalinity for Carbon Sequestration. *Reviews of Geophysics* **2017**, *55* (3), 636–674. https://doi.org/10.1002/2016RG000533.

(5) Wang, H.; Pilcher, D. J.; Kearney, K. A.; Cross, J. N.; Shugart, O. M.; Eisaman, M. D.; Carter, B. R. Simulated Impact of Ocean Alkalinity Enhancement on Atmospheric CO2 Removal in the Bering Sea. *Earth's Future* **2023**, *11* (1), e2022EF002816. https://doi.org/10.1029/2022EF002816.

(6) Eisaman, M. D. Pathways for Marine Carbon Dioxide Removal Using Electrochemical Acid-Base Generation. *Front. Clim.* **2024**, *6*, 1349604. https://doi.org/10.3389/fclim.2024.1349604.

(7) Ringham, M. C.; Hirtle, N.; Shaw, C.; Lu, X.; Herndon, J.; Carter, B. R.; Eisaman, M. D. An Assessment of Ocean Alkalinity Enhancement Using Aqueous Hydroxides: Kinetics, Efficiency, and Precipitation Thresholds. *Biogeosciences* **2024**, *21* (15), 3551–3570. https://doi.org/10.5194/bg-21-3551-2024.

(8) Caserini, S.; Storni, N.; Grosso, M. The Availability of Limestone and Other Raw Materials for Ocean Alkalinity Enhancement. *Global Biogeochemical Cycles* **2022**, *36* (5), e2021GB007246. https://doi.org/10.1029/2021GB007246.

(9) Renforth, P.; Jenkins, B. G.; Kruger, T. Engineering Challenges of Ocean Liming. *Energy* **2013**, *60*, 442–452. https://doi.org/10.1016/j.energy.2013.08.006.

(10) Khoiruddin, K.; Wenten, I. G.; Siagian, U. W. R. Advancements in Bipolar Membrane Electrodialysis Techniques for Carbon Capture. *Langmuir* **2024**, *40* (18), 9362–9384. https://doi.org/10.1021/acs.langmuir.3c03873.

(11) Ropp, R. C. Chapter 2 - Group 17 (H, F, Cl, Br, I) Alkaline Earth Compounds. In *Encyclopedia of the Alkaline Earth Compounds*; Ropp, R. C., Ed.; Elsevier: Amsterdam, 2013; pp 25–104. https://doi.org/10.1016/B978-0-444-59550-8.00002-8.

(12) Zhang, Q.; Awolayo, A. N.; Phelps, P. R.; Vadsariya, S.; Laureijs, C. T.; Eisaman, M. D.; Tutolo, B. M. Enhanced Cation Release via Acid Pretreatment for Gigaton-Scale Geologic CO2 Sequestration in Basalt. *International Journal of Greenhouse Gas Control* **2024**, *139*, 104266. https://doi.org/10.1016/j.ijggc.2024.104266.

(13) Hibbeln, C. F.; Marsh, P.; Myers, C. R.; Valdez, P. J.; Edmundson, S. J.; Subban, C. V. Maximizing Marine Carbon Removal by Coupling Electrochemical and Biological Methods. *Environ. Sci. Technol. Lett.* **2024**, *11* (5), 438–444. https://doi.org/10.1021/acs.estlett.4c00107.

(14) Scott, A.; Oze, C.; Shah, V.; Yang, N.; Shanks, B.; Cheeseman, C.; Marshall, A.; Watson, M. Transformation of Abundant Magnesium Silicate Minerals for Enhanced CO2 Sequestration. *Commun Earth Environ* **2021**, *2* (1), 25. https://doi.org/10.1038/s43247-021-00099-6.

(15) Hamilton, J. L.; Wilson, S.; Morgan, B.; Harrison, A. L.; Turvey, C. C.; Paterson, D. J.; Dipple, G. M.; Southam, G. Accelerating Mineral Carbonation in Ultramafic Mine Tailings via Direct CO2 Reaction and Heap Leaching with Potential for Base Metal Enrichment and Recovery. *Economic Geology* **2020**, *115* (2), 303–323. https://doi.org/10.5382/econgeo.4710.

(16) Qi, Y. The Neutralization and Recycling of Red Mud – a Review. *J. Phys.: Conf. Ser.* **2021**, *1759*, 012004. https://doi.org/10.1088/1742-6596/1759/1/012004.

(17) *BHVO-2 Geochemical Reference Material Information Sheet | U.S. Geological Survey*. https://www.usgs.gov/media/files/bhvo-2-geochemical-reference-material-information-sheet (accessed 2025-07-31).

(18) Lee Pereira, R.; Muangthai, I.; Azimi, A.; Campbell, J.; Delval, M.; Foteinis, S.; Katish, M.; Thonemann, N.; Strunge, T.; Su, D.; Ward, C.; Van der Spek, M.; Renforth, P. *A Framework for Techno-Economic and Life-Cycle Assessment in Ocean Alkalinity Enhancement*; Heriot-Watt University, 2025. https://doi.org/10.17861/v5j0-xw20.

(19) Aromada, S. A.; Eldrup, N. H.; Erik Øi, L. Capital Cost Estimation of CO2 Capture Plant Using Enhanced Detailed Factor (EDF) Method: Installation Factors and Plant Construction Characteristic Factors. *International Journal of Greenhouse Gas Control* **2021**, *110*, 103394. https://doi.org/10.1016/j.ijggc.2021.103394.

(20) Theis, J. *Quality Guidelines for Energy Systems Studies: Cost Estimation Methodology for NETL Assessments of Power Plant Performance*; NETL-PUB--22580, 1567736; 2021; p NETL-PUB--22580, 1567736. https://doi.org/10.2172/1567736.

(21) Zhang, B.; Kroeger, J.; Planavsky, N.; Yao, Y. Techno-Economic and Life Cycle Assessment of Enhanced Rock Weathering: A Case Study from the Midwestern United States. *Environ. Sci. Technol.* **2023**, *57* (37), 13828–13837. https://doi.org/10.1021/acs.est.3c01658.

(22) Strefler, J.; Amann, T.; Bauer, N.; Kriegler, E.; Hartmann, J. Potential and Costs of Carbon Dioxide Removal by Enhanced Weathering of Rocks. *Environ. Res. Lett.* **2018**, *13* (3), 034010. https://doi.org/10.1088/1748-9326/aaa9c4.

(23) Pokrovsky, O. S.; Schott, J. Forsterite Surface Composition in Aqueous Solutions: A Combined Potentiometric, Electrokinetic, and Spectroscopic Approach. *Geochimica et Cosmochimica Acta* **2000**, *64* (19), 3299–3312. https://doi.org/10.1016/S0016-7037(00)00435-X.

(24) Pokrovsky, O. S.; Schott, J. Kinetics and Mechanism of Forsterite Dissolution at 25°C and pH from 1 to 12. *Geochimica et Cosmochimica Acta* **2000**, *64* (19), 3313–3325. https://doi.org/10.1016/S0016-7037(00)00434-8.

(25) Oelkers, E. H.; Declercq, J.; Saldi, G. D.; Gislason, S. R.; Schott, J. Olivine Dissolution Rates: A Critical Review. *Chemical Geology* **2018**, *500*, 1–19. https://doi.org/10.1016/j.chemgeo.2018.10.008.

(26) Morris, P. M.; Wogelius, R. A. Phthalic Acid Complexation and the Dissolution of Forsteritic Glass Studied via *in Situ* FTIR and X-Ray Scattering. *Geochimica et Cosmochimica Acta* **2008**, *72* (8), 1970–1985. https://doi.org/10.1016/j.gca.2008.02.004.

(27) Alexander, G. B.; Heston, W. M.; Iler, R. K. The Solubility of Amorphous Silica in Water. *J. Phys. Chem.* **1954**, *58* (6), 453–455. https://doi.org/10.1021/j150516a002.

(28) Béarat, H.; McKelvy, M. J.; Chizmeshya, A. V. G.; Gormley, D.; Nunez, R.; Carpenter, R. W.; Squires, K.; Wolf, G. H. Carbon Sequestration via Aqueous Olivine Mineral Carbonation: Role of Passivating Layer Formation. *Environ. Sci. Technol.* **2006**, *40* (15), 4802–4808. https://doi.org/10.1021/es0523340.

(29) Johnson, N. C.; Thomas, B.; Maher, K.; Rosenbauer, R. J.; Bird, D.; Brown, G. E. Olivine Dissolution and Carbonation under Conditions Relevant for in Situ Carbon Storage. *Chemical Geology* **2014**, *373*, 93–105. https://doi.org/10.1016/j.chemgeo.2014.02.026.

(30) Czerwinski, F. Critical Minerals for Zero-Emission Transportation. *Materials* **2022**, *15* (16), 5539. https://doi.org/10.3390/ma15165539.

(31) *Mineral Commodity Summaries 2025*; 2025. https://doi.org/10.3133/mcs2025.

(32) Bauer, D.; Khazdozian, H.; Mehta, J.; Nguyen, R.; Severson, M.; Vaagensmith, B.; Toba, L.; Zhang, B.; Hossain, T.; Sibal, A.; Smith, B.; Riddle, M.; Graziano, D.; Mathew, T.; Cuscaden, P.; Dai, Q.; Iloeje, C.; Edgemon, L.; Sarna, C.; Quaresima, J. *2023 Critical Materials Strategy*; INL/RPT--23-72323-Rev.001, 1998242; 2023; p INL/RPT--23-72323-Rev.001, 1998242. https://doi.org/10.2172/1998242.

(33) Reich, M.; Simon, A. C. Critical Minerals. *Annual Review of Earth and Planetary Sciences* **2025**, *53* (Volume 53, 2025), 141–168. https://doi.org/10.1146/annurev-earth-040523-023316.

(34) Ragan, D. M. Emplacement of the Twin Sisters Dunite, Washington. *American Journal of Science* **1963**, *261* (6), 549–565. https://doi.org/10.2475/ajs.261.6.549.

(35) Krevor, S. C.; Graves, C. R.; Van Gosen, B. S.; McCafferty, A. E. *Mapping the Mineral Resource Base for Mineral Carbon-Dioxide Sequestration in the Conterminous United States: U.S. Geological Survey Digital Data Series 414*; Data Series; Data Series; 2009.

(36) *Global Gravel, Pebbles, and Crushed Stone Market: Market Volume Expected to Reach 12,843M Tons by 2035, with Market Value Forecasted at $648.6B - News and Statistics - IndexBox*. https://www.indexbox.io/blog/gravel-pebbles-and-crushed-stone-for-concrete-and-road-aggregates-world-market-overview-2024-2/ (accessed 2025-07-31).

(37) Sun, X. Supply Chain Risks of Critical Metals: Sources, Propagation, and Responses. *Front. Energy Res.* **2022**, *10*. https://doi.org/10.3389/fenrg.2022.957884.

(38) Nakajima, K.; Otsuka, Y.; Iwatsuki, Y.; Nansai, K.; Yamano, H.; Matsubae, K.; Murakami, S.; Nagasaka, T. Global Supply Chain Analysis of Nickel: Importance and Possibility of Controlling the Resource Logistics. *Metall. Res. Technol.* **2014**, *111* (6), 339–346. https://doi.org/10.1051/metal/2014036.

(39) Nieto, A.; Montaruli, V.; Cardu, M. Strategic Approach for Nickel Future Supply. In *TRANSACTIONS OF THE SOCIETY FOR MINING, METALLURGY, AND EXPLORATION*; SOCIETY FOR MINING, METALLURGY, AND EXPLORATION, 2013; Vol. 334, pp 510–518.

(40) Kalantzakos, S. The Race for Critical Minerals in an Era of Geopolitical Realignments. *The International Spectator* **2020**, *55* (3), 1–16. https://doi.org/10.1080/03932729.2020.1786926.

(41) Ansari, T. M.; Marr, I. L.; Tariq, N. Heavy Metals in Marine Pollution Perspective–A Mini Review. *J. of Applied Sciences* **2003**, *4* (1), 1–20. https://doi.org/10.3923/jas.2004.1.20.

(42) Hunt, J. W.; Anderson, B. S.; Phillips, B. M.; Tjeerdema, R. S.; Puckett, H. M.; Stephenson, M.; Tucker, D. W.; Watson, D. Acute and Chronic Toxicity of Nickel to Marine Organisms: Implications for Water Quality Criteria. *Environmental Toxicology and Chemistry* **2002**, *21* (11), 2423–2430. https://doi.org/10.1002/etc.5620211122.

(43) Blais, J. F.; Djedidi, Z.; Cheikh, R. B.; Tyagi, R. D.; Mercier, G. Metals Precipitation from Effluents: Review. *Practice Periodical of Hazardous, Toxic, and Radioactive Waste Management* **2008**, *12* (3), 135–149. https://doi.org/10.1061/(ASCE)1090-025X(2008)12:3(135).

(44) Buffalo Reef Responsiveness Summary March 2024. https://www.michigan.gov/dnr/-/media/Project/Websites/dnr/Documents/Fisheries/BuffaloReef/Buffalo-Reef-Responsiveness-Summary_March-2024.pdf?rev=8571a4fcc74f42f78afeb2f5868bb626&hash=744B9395DF962F05DFFF7993C73DF785 (accessed 2025-07-31).

(45) Bana, I. S.; Wan, W.; Shen, L. Optimization of High-Pressure Acid Leaching for Nickel and Cobalt Recovery from Ultralow-Grade Laterite Ores. *JOM* **2025**, *77* (7), 5192–5204. https://doi.org/10.1007/s11837-025-07402-2.

(46) de Oliveira, R. P.; da Conceição do Nascimento, R.; Feldhagen, H. G. Agglomeration and Characterization of Nickel Concentrate (MHP) Pellets for Ferronickel Production. *Mining, Metallurgy & Exploration* **2020**, *37* (5), 1653–1665. https://doi.org/10.1007/s42461-020-00235-4.

(47) Sahiruddin, S.; Liu, W.; Li, B.; Zhang, K.; Zhang, Z.; Liu, F. Thermodynamics Analysis and Experimental Optimization of Mixed Hydroxide Precipitation from Nickel Laterite Ores. *Mining, Metallurgy & Exploration* **2025**. https://doi.org/10.1007/s42461-025-01276-3.

(48) Jones, A. N.; Welham, N. J. Properties of Aged Mixed Nickel–Cobalt Hydroxide Intermediates Produced from Acid Leach Solutions and Subsequent Metal Recovery. *Hydrometallurgy* **2010**, *103* (1), 173–179. https://doi.org/10.1016/j.hydromet.2010.03.017.

(49) Mulat Muhammud, A.; Kumar Gupta, N. Nanostructured SiO 2 Material: Synthesis Advances and Applications in Rubber Reinforcement. *RSC Advances* **2022**, *12* (29), 18524–18546. https://doi.org/10.1039/D2RA02747J.

(50) Abdellaoui, I.; Islam, M. M.; Sakurai, T.; Hamzaoui, S.; Akimoto, K. Impurities Removal Process for High-Purity Silica Production from Diatomite. *Hydrometallurgy* **2018**, *179*, 207–214. https://doi.org/10.1016/j.hydromet.2018.06.009.

(51) Harvey, R.; Hannah, R.; Vaughan, J. Selective Precipitation of Mixed Nickel–Cobalt Hydroxide. *Hydrometallurgy* **2011**, *105* (3), 222–228. https://doi.org/10.1016/j.hydromet.2010.10.003.

(52) Rath, M.; Behera, L. P.; Dash, B.; Sheik, A. R.; Sanjay, K. Recovery of Dimethylglyoxime (DMG) from Ni-DMG Complexes. *Hydrometallurgy* **2018**, *176*, 229–234. https://doi.org/10.1016/j.hydromet.2018.01.014.

(53) Bartzas, G.; Komnitsas, K. Cradle to Gate Life-Cycle Assessment of Battery Grade Nickel Sulphate Production through High-Pressure Acid Leaching. *Science of The Total Environment* **2024**, *952*, 175902. https://doi.org/10.1016/j.scitotenv.2024.175902.

(54) Norgate, T.; Jahanshahi, S. Assessing the Energy and Greenhouse Gas Footprints of Nickel Laterite Processing. *Minerals Engineering* **2011**, *24* (7), 698–707. https://doi.org/10.1016/j.mineng.2010.10.002.

(55) Gu, S.; Yang, L.; Liang, X.; Zhou, J. Life Cycle Assessment and Process Optimization of Precipitated Nanosilica—A Case Study in China. *Energies* **2024**, *17* (22), 5621. https://doi.org/10.3390/en17225621.

(56) Drummond, C.; McCann, R.; Patwardhan, S. V. A Feasibility Study of the Biologically Inspired Green Manufacturing of Precipitated Silica. *Chemical Engineering Journal* **2014**, *244*, 483–492. https://doi.org/10.1016/j.cej.2014.01.071.

(57) Grbeš, A. A Life Cycle Assessment of Silica Sand: Comparing the Beneficiation Processes. *Sustainability* **2016**, *8* (1), 11. https://doi.org/10.3390/su8010011.

(58) Gan, Y.; Griffin, W. M. Analysis of Life-Cycle GHG Emissions for Iron Ore Mining and Processing in China—Uncertainty and Trends. *Resources Policy* **2018**, *58*, 90–96. https://doi.org/10.1016/j.resourpol.2018.03.015.

(59) U.S. Geological Survey, Leetown Science Center, Kearneysville, WV 25430; Sibrell, P. L.; Wildeman, T. R.; Frienmuth, M.; Chambers, M.; Bless, D. DEMONSTRATION OF A PULSED LIMESTONE BED PROCESS FOR THE TREATMENT OF ACID MINE DRAINAGE AT THE ARGO TUNNEL SITE, IDAHO SPRINGS, COLORADO. *JASMR* **2005**, *2005* (1), 1068–1081. https://doi.org/10.21000/JASMR05011068.

Supporting Information

Table S1. Parameter values used for base case scenario in techno-economic analysis.

Parameter Name	Value	Units	Notes
Project Lifespan	40	Years	
Capacity Factor	80	%	
Cost of electricity	0.0646	USD kWh^{-1}	Price of industrial electricity in WA
CO_2 intensity of electricity	0.1324	kgCO2 kWh^{-1}	Average grid CO_2 emissions for WA electricity in 2023
Gross CDR capacity	50581	tCDR yr^{-1}	Assumed as a basis for the process model
Acid Production Ratio	40657	L acid $tCDR^{-1}$	Assumes 78% OAE efficiency, and includes losses from NaOH use for precipitation
Acid Strength	0.809	eq L^{-1}	Value within typical concentration range for BPMED OAE processes
EPC Rate Factor	15	%	From Lee Pereira, R. et al. (2025)
Process Contingency Factor	50	%	Recommendation from Lee Pereira, R. et al. (2025), and Theis, J. (2021) for TRL 4 process
Project Contingency Factor	15	%	Recommendation from Lee Pereira, R. et al. (2025) for preliminary design
Owners Cost Spare Parts Factor	0.5	%	Recommendation from Theis, J. (2021)
Financing Cost Factor	2.7	%	Recommendation from Theis, J. (2021)
Additional Start-up capital Factor	2	%	Recommendation from Theis, J. (2021)
Other Owners Costs Factor	15	%	Recommendation from Theis, J. (2021)
Operator Salary	52000	USD yr^{-1}	Estimate from salary websites for process operator role in WA
Total Maintenance Cost Factor	1.5	%	Recommendation from Lee Pereira, R. et al. (2025)
Maintenance Labor Factor	40	%	Recommendation from Lee Pereira, R. et al. (2025)
Maintenance Materials Factor	60	%	Recommendation from Lee Pereira, R. et al. (2025)
Administrative Labor Factor	20	%	Recommendation from Lee Pereira, R. et al. (2025)
Insurance and Property Taxes Factor	1	%	Recommendation from Lee Pereira, R. et al. (2025)
Discount Rate	8	%	
Transport Distance	90.75	km	Distance from Twin Sisters mine to Anacortes, WA
Min., Prod., Comm. Price	41	USD $tRock^{-1}$	From Strefler, J. et al. (2018), for rock comminution to an average particle diameter of 10 microns
Waste Disposal Fee	75	USD $tonne^{-1}$	Estimate for landfill fees, based on various townships in WA state
Prec-1 Value	-200	USD $tonne^{-1}$	Based on selling as commercial grade silica, but largely discounted (80% reduction) to account for product purity
Prec-2 Value	-105	USD $tonne^{-1}$	Price for average grade commodity iron ore
Prec-3 Value	-7360	USD $tonne^{-1}$	Based on price that various purity levels of MHP can fetch on market

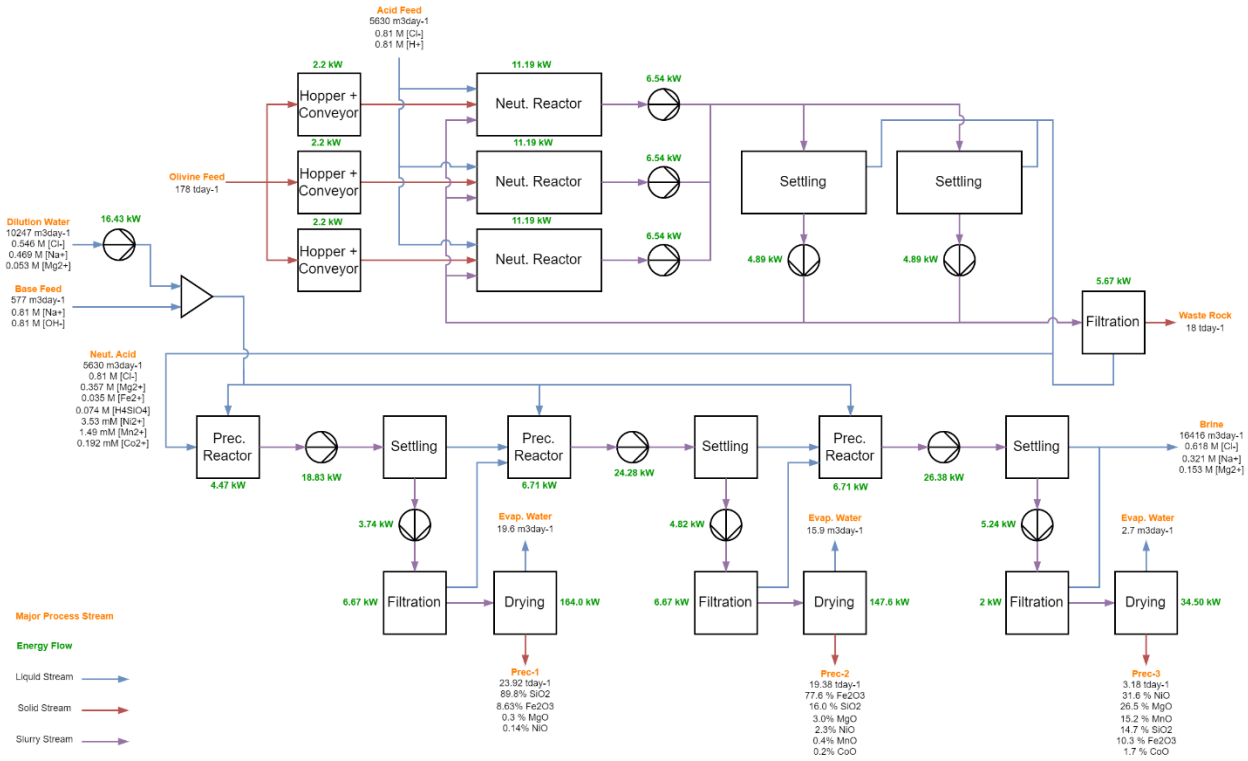

Figure S1. Process flow diagram for the process model used in the techno-economic analysis, including mass balance information for key process streams, and energy flows required to run process equipment.